

Atom-molecule conversion with particle losses

B. Cui, L. C. Wang, X. X. Yi

*School of Physics and Optoelectronic Technology,
Dalian University of Technology, Dalian 116024, China*

(Dated: November 10, 2021)

Based on the mean-field approximation and the phase space analysis, we study the dynamics of an atom-molecule conversion system subject to particle loss. Starting from the many-body dynamics described by a master equation, an effective nonlinear Schrödinger equation is introduced. The classical phase space is then specified and classified by fixed points. The boundary, which separate different dynamical regimes have been calculated and discussed. The effect of particle loss on the conversion efficiency and the self-trapping is explored.

PACS numbers: 03.65.Bz, 07.60.Ly

I. INTRODUCTION

Association of ultracold atoms into molecules is currently an active topic in the field of ultracold quantum physics, it attracts much attention due to its important applications ranging from the production of molecular Bose-Einstein condensates to the search for the permanent electric dipole moment, see for example [1–12]. By applying a time varying magnetic field in the vicinity of Feshbach resonance, a pair of atoms can bound into a diatomic molecule [13, 14], this conversion can be described by the Gross-Pitaevski (GP) equations within the mean-field theory (MFT) [15–20]. Such an treatment reduces the full many-body problem into a set of coupled nonlinear Schrödinger equations and the complicated many-body dynamics is then turned into a two-mode dynamics. Earlier study shows that the nonlinearity, which arises from both the atom-atom and molecule-molecule couplings, plays an important role in the system. Four distinct regimes, each has different feature in dynamics can be classified, accordingly the bifurcation of the fixed points in the classical phase space [16, 20] is identified.

Decoherence that arises from the unavailable coupling between the environment (thermal atoms or molecules) and the condensed system plays an important role in atomic or molecular Bose-Einstein condensate [21–26]. Description of decoherence by fully including the quantum effects requires sophisticated theoretical studies, however the standard approach in quantum optics can reduce the complexity and in fact it has been widely used in Bose-Einstein condensates [27–32]. For an atom-molecule conversion system, we then ask: will the decoherence effect be different from that in the pure atomic or molecular Bose-Einstein condensates? What are the fixed points in this situation? How do these fixed points behave? We will answer these questions in this paper.

In this paper, we focus on the amplitude decoherence (particle loss), which may arise from inelastic collision between condensate and noncondensate particles in the system. The standard approach in quantum optics for open systems are used and the master equation is derived by treating the noncondensate atoms and molecules as a Markovian reservoir. Under the mean-field approxima-

tion, an effective non-Hermitian Gross-Pitaevskii equation is derived. Bifurcation of the fixed points divides the parameter space into different dynamical regimes, boundaries that separate these regimes are changed by the decoherence. By calculating the corresponding Jacobian matrix, we find that a sudden transition in the fixed point from elliptic point to attractor or repeller happens with non-zero decoherence rate, which reflects the meta-stable features of the system under the decoherence. The atom-molecule conversion efficiency for the molecular condensate as well as the self-trapping are also studied.

The paper is organized as follows. In Sec. II, we introduce the model and transform the master equation to a non-Hermitian nonlinear Schrödinger equation. Conditions that determine the fixed points are derived. In Sec. III, we define different regimes by the bifurcation of the fixed points and study the dynamics of system in these regimes. In Sec. IV, we investigate the effect of particle loss on the conversion efficiency. In Sec. V, we shed light on the self-trapping taking the decoherence into account, an explanation for the observed features is given in the framework of mean-field theory. Finally, we conclude our results in Sec. VI.

II. MODEL

Based on the two-mode approximation, the Hamiltonian that includes the atom-atom collision U_{aa} , atom-molecule conversion with rate V , and molecule-molecule couplings U_{bb} takes the following form [16, 17]

$$H = \mu_a \hat{a}^\dagger \hat{a} + \mu_b \hat{b}^\dagger \hat{b} + U_{aa} \hat{a}^\dagger \hat{a}^\dagger \hat{a} \hat{a} + U_{bb} \hat{b}^\dagger \hat{b}^\dagger \hat{b} \hat{b} + U_{ab} \hat{a}^\dagger \hat{a} \hat{b}^\dagger \hat{b} + V(\hat{a}^\dagger \hat{a}^\dagger \hat{b} + \hat{b}^\dagger \hat{a} \hat{a}). \quad (1)$$

The master equation [33] that takes the particle loss into account can be derived as in the textbook [21],

$$\dot{\rho} = -i[\hat{H}, \rho] - \frac{\Gamma_a}{2}(\hat{a}^\dagger \hat{a} \rho + \rho \hat{a}^\dagger \hat{a} - 2\hat{a} \rho \hat{a}^\dagger) - \frac{\Gamma_b}{2}(\hat{b}^\dagger \hat{b} \rho + \rho \hat{b}^\dagger \hat{b} - 2\hat{b} \rho \hat{b}^\dagger), \quad (2)$$

where Γ_a and Γ_b represent decoherence rates for atomic and molecular modes, respectively. In the mean-field approximation, the quantum fluctuation is negligible. It is appropriate to replace \hat{a} and \hat{b} with c numbers $a = |a|e^{i\theta_a}$ and $b = |b|e^{i\theta_b}$. With these considerations, the master equation (2) can be casted into the following nonlinear Schrödinger equation,

$$i\frac{d}{dt}\begin{pmatrix} a \\ b \end{pmatrix} = H\begin{pmatrix} a \\ b \end{pmatrix}, \quad (3)$$

$$H = \begin{pmatrix} R - Uz - \frac{i}{2}\Gamma_a & 2Va^* \\ Va & -2R + 2Uz - \frac{i}{2}\Gamma_b \end{pmatrix}, \quad (4)$$

with $z = |a|^2 - 2|b|^2$ describing the number difference for atoms in the two modes. $U = \frac{1}{4}U_{ab} - \frac{1}{2}U_{aa} - \frac{1}{8}U_{bb}$ represents a coupling strength and V is the conversion rate. $R = \frac{1}{4}(2\mu_a - \mu_b + 2U_{aa} - \frac{1}{2}U_{bb})$ denotes the energy difference between the two modes, which can be effectively tuned by a time-varying external field [17, 18]. Here and hereafter, we rescale R, U, Γ_a, Γ_b in units of V , and t in units of $1/V$, $\hbar = 1$ has been set, hence all parameters in this paper are of dimensionless.

Similar to the two-mode Bose-Hubbard model, the projective Hilbert space for such an atom-diatomic molecule conversion system can be spanned by a set of Bloch vectors. Under the mean-field approximation, the Bloch vectors can be written as [19]

$$\mathbf{h} = (2\sqrt{2}Re[(a^*)^2b], 2\sqrt{2}Im[(a^*)^2b], |a|^2 - 2|b|^2). \quad (5)$$

With the normalization condition $|a|^2 + 2|b|^2 = 1$, the projective space is a tear-drop shaped surface as shown in Fig. 2.

To analyze the dissipative dynamics of the system in its classical phase space, we define relative phase θ , particle number n and normalized population difference S as

$$\theta = 2\theta_a - \theta_b, \quad (6)$$

$$n = 2|b|^2 + |a|^2, \quad (7)$$

$$S = \frac{z}{n}. \quad (8)$$

Inserting these definitions into Eq. (3), a set of evolution equations is obtained

$$\dot{S} = -2V\sqrt{n}(1+S)\sqrt{1-S}\sin\theta - \Gamma_-(1-S^2), \quad (9)$$

$$\dot{\theta} = 4UnS - 4R - V\sqrt{n}\frac{1-3S}{\sqrt{1-S}}\cos\theta, \quad (10)$$

$$\dot{n} = -(\Gamma_+ + \Gamma - S)n, \quad (11)$$

with $\Gamma_+ = \frac{1}{2}(\Gamma_a + \Gamma_b)$ and $\Gamma_- = \frac{1}{2}(\Gamma_a - \Gamma_b)$ representing the total and relative decoherence rates for the two modes, respectively. Ignoring the coupling between the system and its environment ($\Gamma_a = \Gamma_b = 0$), the dynamics of the system can be described by an effective Hamiltonian as

$$H = 2V(1+S)\sqrt{1-S}\cos\theta - 2US^2 + 4RS. \quad (12)$$

It is found that the bifurcation of the fixed points falls into four regimes in the parameter space [16, 20] as shown in Fig. 1. Due to inelastic collisions between particles in the condensates and that in the thermal cloud, the loss of atoms and molecules as one source of decoherence is unavoidable in practices. Thus it is interesting and desired to study the dynamics of this system with decoherence. By the standard procedure used in non-Hermitian system [27, 31], we study the dynamics of the system with notations $C = Un$, $\Omega = V\sqrt{n}$. With these knowledge, the effects of the particle loss on the dynamics as well as the features of fixed point can be clearly revealed in classical phase space. For simplicity, in the following discussion, we set $\Gamma = \Gamma_-$ and rewrite the equations for the population difference and relative phase as

$$\dot{S} = -2\Omega(1+S)\sqrt{1-S}\sin\theta - \Gamma(1-S^2), \quad (13)$$

$$\dot{\theta} = 4CS - 4R - \Omega\frac{1-3S}{\sqrt{1-S}}\cos\theta. \quad (14)$$

The fixed points of the system are determined by

$$\dot{S} = \dot{\theta} = 0. \quad (15)$$

To be specific, the fixed points on the boundary are $S = -1$, $\theta = \arccos(-\frac{\sqrt{2}(C+R)}{\Omega})$, while the other fixed points are determined by

$$\begin{aligned} & (9\Gamma^2 + 64C^2)S^3 - (\Gamma^2 - 4\Omega^2 + 64R^2) \\ & - (15\Gamma^2 - 36\Omega^2 + 64C^2 + 128CR)S^2 \\ & - (24\Omega^2 - 7\Gamma^2 - 64R^2 - 128CR)S = 0, \end{aligned} \quad (16)$$

$$\sin\theta = -\frac{\Gamma}{2\Omega}\sqrt{1-S}. \quad (17)$$

Through a Jacobian matrix defined by

$$J = \begin{pmatrix} \partial\dot{S}/\partial S & \partial\dot{S}/\partial\theta \\ \partial\dot{\theta}/\partial S & \partial\dot{\theta}/\partial\theta \end{pmatrix}, \quad (18)$$

we can study the stability of the fixed points as did in the literature [32, 34, 35].

From Eqs. (13) and (14), we find that the dynamics of the system depends only on the relative decoherence rate Γ , but not on the total decoherence rate. The total decoherence rate affect the system through $n = n_0e^{-\Gamma_+t}$. With zero relative decoherence rate ($\Gamma = 0$), the effective Hamiltonian can be written as

$$H = 2\Omega(1+S)\sqrt{1-S}\cos\theta - 2CS^2 + 4RS, \quad (19)$$

which differs from the case without decoherence only at the conversion amplitude Ω and coupling strength C . In the next section, we shall discuss the effect of relative decoherence rate on the dynamics of the system.

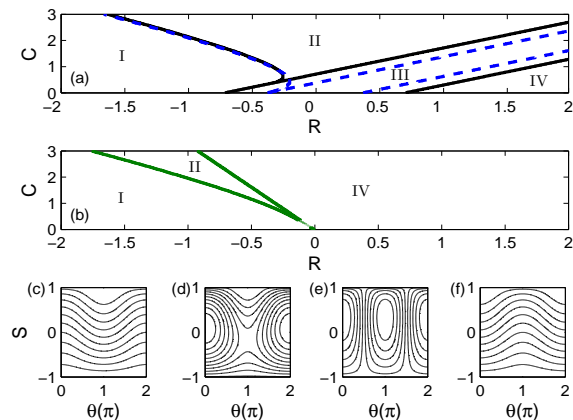


FIG. 1: (color online) Parameter space spanned by nonlinearity C and energy difference R . Different regimes are distinguished by boundary lines, where black solid lines represent the case for $\Gamma = 0$, while blue dashed lines denotes the case for $\Gamma = 1.2$ in (a). Green solid lines in (b) denotes the boundary lines for $\Gamma = 2.4$. (c), (d), (e), and (f) describe the classical phase space for region I , II , III , and IV , respectively.

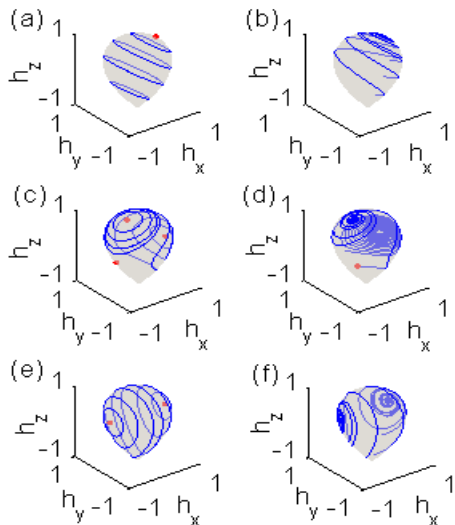


FIG. 2: (color online) Mean-field dynamics on the Bloch sphere for Hermitian (left) and non-Hermitian (right) cases. The north pole and south pole of the sphere corresponds to the pure atomic condensate and the pure molecular condensate, respectively. Red spots and center of the vortex denote the location of the fixed points. Blue solid lines represent the trajectories for the time evolution of the system. Parameters chosen are $R = 1, U = 0$ for (a) and (b), $R = 0, U = 2$ for (c) and (d), and $R = 0, U = 0$ for (e) and (f). The spheres on left side ((a),(c),(e)) describe decoherence free case ($\Gamma = 0$), while the spheres on right side depict the decoherence case ($\Gamma = 1$).

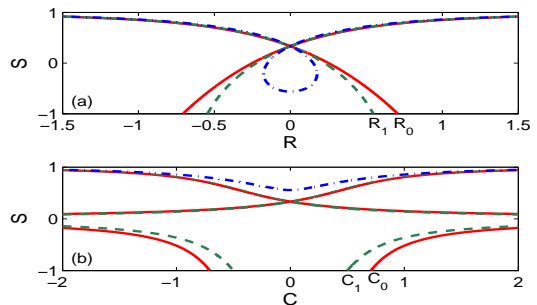


FIG. 3: (color online) (a) Locations of fixed points for different decoherence rate Γ and energy difference R . Parameters chosen are $U = 0, V = 1$, and $\Gamma = 0, 0.9, 1.6$ for red solid line, green dashed line and blue dotted line, respectively. (b) Locations of fixed points for different decoherence rate Γ and interaction strength C . Parameters chosen are $R = 0, V = 1$, and $\Gamma = 0, 0.5, 1.5$ for red solid line, green dashed line and blue dotted line, respectively.

III. FOUR DYNAMICAL REGIMES WITH DECOHERENCE

In Ref. [16], without considering the decoherence effect, by the feature of fixed points, the parameter space was divided into four regions. Here we re-divide the region by taking the decoherence into account (see Fig. 1 and Fig. 2). Boundaries that separate different regions, are determined by numerically solving Eqs. (16,17). Note that the fixed points on the boundary behave like the fixed points in the region labeled by a smaller number (e.g. boundary that separate regions I and II belongs to the region I).

Figure 1(c) shows Poincaré section of the classical Hamiltonian for the region I . The only fixed point is located near the boundary of the phase space ($S = 1$) and the dynamics of the system is localized. When taking the decoherence into consideration, the fixed point near $S = 1$ turns into an attractor, where Figs. 2(a) and 2(b) show trajectories on the tear-drop shaped Bloch sphere. The dynamics of the system becomes delocalized due to the appearance of such an attractor.

By changing the energy difference R and the nonlinearity C (see Fig. 1(a)), the system can go across the boundary into region II , the fixed point in region I bifurcates into two elliptic points and a hyperbolic one as Fig. 1(d) shows. The region II shares similar features with the self-trapping in the two-mode Bose-Hubbard model [36, 37]. With a negative decoherence rate, both of the two elliptic fixed points transit to attractors in this region (see Figs. 2(c) and 2(d)). While the locations of the stable attractors are just slightly changed due to the decoherence (see Fig. 3(b)).

Figure 1(e) illustrates the Poincaré section of the classical Hamiltonian for region III without decoherence. In this region, large amplitude oscillations around the elliptic fixed can be observed, see Fig. 2(e). With $U = 0$ and

$R = 0$, the location of the fixed points in this region can be derived analytically

$$(S, \theta) = \left(\frac{1}{3}, \pi + \arcsin\left(\frac{\Gamma}{\sqrt{6}\Omega}\right), \frac{1}{3}, 2\pi - \arcsin\left(\frac{\Gamma}{\sqrt{6}\Omega}\right) \right), \quad (20)$$

where we assume the decoherence rate positive, and the relative phase was restricted in $\theta \in [0, 2\pi]$. From Eq. (20), we find that in addition to the feature changes of the fixed points, the relative phase between the two fixed points decreases and the fixed points becomes asymmetric due to the decoherence as shown in Fig. 2(f). As the decoherence rate increases, the area of regime *III* is compressed (see blue dashed line in Fig. 1(a)). The two boundaries coincides and region *III* vanishes (see dash dotted line in Fig. 3(a)), when decoherence rate is larger than a threshold ($\Gamma > \sqrt{2}\Omega$), a hyperbolic fixed point arises from the bottom of the phase space (see dash-dotted line in Fig. 3(a)). The boundary that separates regions *III* and *IV* is shifted due to decoherence. This boundary shift can be explained as a threshold decrease in the energy difference R (denoted by R_0 and R_1 in Fig. 3(a)), which is a witness for the bifurcation of fixed points in classical phase space.

The dynamics in region *IV* behaves similarly as that in region *I*. The elliptic fixed point turns into an attractor due to negative decoherence rate, the dynamics in this region then becomes delocalized (see Figs. 2(a) and 2(b)).

Next, we focus on the changes of the fixed points. Such a change in classical phase space is fundamental for non-hermitian Bose-Hubbard system [27, 31, 32]. However, we find that, in the atom-molecule conversion system, the change differs from Bose-Hubbard model in two respects. Firstly, the type of the fixed point (a repeller or an attractor) is determined by the the sign of decoherence rate Γ and the location of the fixed point S . If Γ and S are different in sign, i.e., one of them is positive while another is negative, the original elliptic fixed point transits into a stable attractor. Otherwise, the original fixed point turns into an unstable repeller. Secondly, the transition is *sudden*, in other words, the transition happens provided the decoherence rate is not zero. This is different from the decoherence effect on Bose-Einstein condensates in a double-well potential, namely there exists a critical value for the decoherence rate [27]. In the atom-molecule conversion system, the transition happens once the decoherence exists, regardless of how small the decoherence being. The phenomenon reflects not only the meta-stable behavior of the open many-particle system, but also the sensitivity of the atom-molecule conversion system to particle loss.

IV. CONVERSION EFFICIENCY FOR MOLECULAR CONDENSATE

In experiments, the association of ultracold atoms into diatomic molecules can be achieved by applying a time-

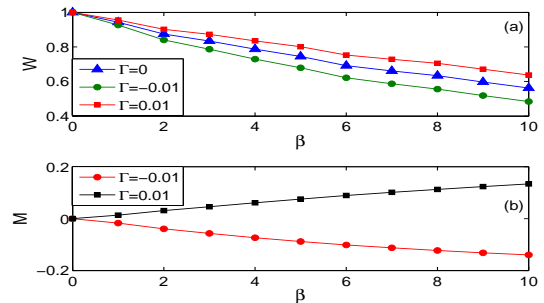


FIG. 4: (color online) Conversion efficiency W in (a) and relative efficiency M in (b) as a function of the sweeping rate β under different decoherence rate Γ .

dependent magnetic field in the vicinity of a Feshbach resonance, which corresponds to the change between different regimes ($I \rightarrow III \rightarrow IV$) in the parameter space (see Fig. 1). To examine the effect of decoherence on the conversion process, we define conversion efficiency, relative efficiency and sweeping rate of the external field as

$$W = \frac{|b(T)|^2}{n(T)}, \quad (21)$$

$$M = \frac{W(\Gamma) - W(0)}{W(0)}, \quad (22)$$

$$\beta = \dot{R}, \quad (23)$$

where T denotes the terminal time for the conversion, $W(\Gamma)$ and $W(0)$ denote the conversion efficiency with and without decoherence, respectively. M describes the relative increases or decreases of the efficiency between decoherence and decoherence-free case. By adjusting the external magnetic field [17], R can be linearly manipulated to across the Feshbach resonance point ($R = R_0 + \beta t$, $R_0 = \beta T$, $t \in [0, T]$), until the system relaxes into a steady state. The conversion efficiency with decoherence can be calculated with the same parameters except the decoherence rate. Here we choose the initial state of the system to be in pure atomic mode ($|a(0)|^2 = 1$).

The results of W show that conversion efficiency increases with positive decoherence rate. While a negative decoherence rate decreases the conversion efficiency (see Fig. 4). This can be interpreted by the appearance of attractor or repeller in the phase space. With a negative decoherence rate, the elliptic fixed points near the atomic mode turns into an attractor and the atoms are attracted to stay away from molecular mode. (see Figs. 2(b) and 2(f)). The conversion process is depressed by such an attractor and the conversion efficiency decreases. Similarly, a positive decoherence rate will increase the conversion efficiency.

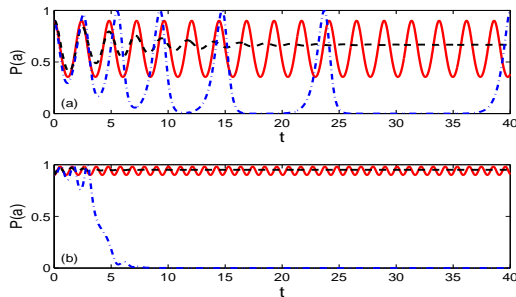


FIG. 5: (color online) Time evolution for the population of atomic mode $P(a) = |a(t)|^2$ under different decoherence rates as $\Gamma = 0, -0.5, 0.5$ denoted by red solid line, black dashed line and blue dash-dotted line both in (a) and (b). Parameters chosen are $V = 1, R = 0$ for both (a) and (b), $U = 0$ for (a) and $U = 1.5$ for (b). The initial population for atoms are $|a(0)|^2 = 0.9$.

V. TUNNELING AND SELF-TRAPPING

In this section, we investigate the effect of particle loss on the dynamics of the system, the atoms may oscillates between atomic and molecular modes (corresponding to regime III), and they can also be trapped in one of the modes (corresponding to the regime II in parameter space).

In regime III, the atoms oscillate between atomic mode and molecular mode (see Fig. 2(e)). When the relative decoherence rate is positive, the fixed point transits from elliptic to a repeller, the amplitude of the oscillation is then increased (see dash dotted line in Fig. 5(a)). While for negative relative decoherence rate, the oscillation is compressed, since the elliptic fixed point suddenly transits to an attractor (see dashed line in Fig. 5(a)).

With C increases, the dynamics of the system turns into the self-trapping regime, which belongs to the regime

II in Fig. 1(a). We find that the threshold of the coupling constant is decreased by the decoherence, i.e., the decoherence supports the self-trapping (denoted by C_0 and C_1 in Fig. 3(b)). With negative relative decoherence rate, the fixed point near the atomic mode transits into an attractor. The self-trapping in atomic mode keeps (see black dashed line in Fig. 5(b)). When the relative decoherence rate is positive, which indicates a repeller in the phase space, the self-trapping in atomic mode is ruined, because the atoms are repelled and converted into molecules, as dash dotted line shows in Fig. 5(b).

A physics understanding is coming

VI. CONCLUSION

In summary, we have investigated the effect of particle loss on the dynamics of the atom-molecule conversion system. Within the mean-field approximation, the classical phase space is specified and the fixed points are calculated. Due to the bifurcation of the fixed points in the phase space, the parameter space can be divided into different regimes. We find that the boundary, which separates different regimes are changed by the decoherence. A sudden transition for the fixed points from elliptic to attractor or repeller happens. Such a transition not only reflects the meta-stable behavior of the system, but also characterizes the phase-space structure of the atom-molecule conversion system. The effect of decoherence on the conversion efficiency and the self-trapping is explored with the mean-field approximation.

This work is supported by NSF of China under grant Nos 61078011 and 10935010, the Open Research Fund of State Key Laboratory of Precision Spectroscopy, East China Normal University, as well as the National Research Foundation and Ministry of Education, Singapore under academic research grant No. WBS: R-710-000-008-271.

-
- [1] D. J. Heinzen, R. Wynar, P. D. Drummond, and K. V. Kheruntsyan, *Phys. Rev. Lett.* **84**, 5029 (2000).
 - [2] E. Donley, N. Claussen, S. Thompson, and C. Wieman, *Nature (London)* **417**, 529 (2002).
 - [3] J.J. Hudson, B.E. Sauer, M.R. Tarbutt, E.A. Hinds, *Phys. Rev. Lett.* **89**, 023003 (2002).
 - [4] M. Greiner, C. A. Regal, and D. S. Jin, *Nature (London)* **426**, 537 (2003).
 - [5] S. Jochim, M. Bartenstein, A. Altmeyer, G. Hendl, S. Riedl, C. Chin, J. Hecker Denschlag, and R. Grimm, *Science* **302**, 2101 (2003).
 - [6] M. W. Zwerlein, C. A. Stan, C. H. Schunck, S. M. F. Raupach, S. Gupta, Z. Hadzibabic, and W. Ketterle, *Phys. Rev. Lett.* **91**, 250401 (2003).
 - [7] A. P. Hines, R. H. McKenzie, and G. J. Milburn, *Phys. Rev. A* **67**, 013609 (2003).
 - [8] C.A. Regal, M. Greiner, D.S. Jin, *Phys. Rev. Lett.* **92**, 040403 (2004).
 - [9] P. Naidon, E. Tiesinga, and P. S. Julienne, *Phys. Rev. Lett.* **100**, 093001 (2008).
 - [10] M. Junker, D. Dries, C. Welford, J. Hitchcock, Y. P. Chen, and R. G. Hulet, *Phys. Rev. Lett.* **101**, 060406 (2008).
 - [11] H. Jing, Y. G. Deng, and W. P. Zhang, *Phys. Rev. A* **80**, 025601 (2009).
 - [12] J. Qian, W. P. Zhang, and H. Y. Ling, *Phys. Rev. A* **81**, 013632 (2010).
 - [13] E. Timmermans et al., *Phys. Rep.* **315**, 199 (1999).
 - [14] T. Köhler, K. Góral, and P. S. Julienne, *Rev. Mod. Phys.* **78**, 1311 (2006).
 - [15] A. Vardi, V. A. Yurovsky, and J. R. Anglin, *Phys. Rev. A* **64**, 063611 (2001).
 - [16] G. Santos, A. P. Tonel, A. Foerster, and J. Links, *Phys. Rev. A* **73**, 023609 (2006).

- [17] J. Li, D.-F. Ye, C. Ma, L.-B. Fu, and J. Liu, Phys. Rev. A **79**, 025602 (2009).
- [18] B. Liu, L.-B. Fu, and J. Liu, Phys. Rev. A **81**, 013602 (2010).
- [19] L.-B. Fu and J. Liu, Annals of Physics, **325**, 2425 (2010).
- [20] G. Santos, A. Foerster, J. Links, E. Mattei, and S. R. Dahmen Phys. Rev. A **81**, 063621 (2010).
- [21] J. Anglin, Phys. Rev. Lett. **79**, 6 (1997).
- [22] J. Ruostekoski and D. F. Walls, Phys. Rev. A **58**, R50 (1998).
- [23] A. Vardi and J. R. Anglin, Phys. Rev. Lett. **86**, 568 (2001).
- [24] J. R. Anglin and A. Vardi, Phys. Rev. A **64**, 013605 (2001).
- [25] W Wang, L. B. Fu, and X. X. Yi, Phys. Rev. A **75**, 045601 (2007).
- [26] N. Syassen, D. M. Bauer, M. Lettner, T. Volz, D. Dietze, J. J. García-Ripoll, J. I. Cirac, G. Rempe, and S. Dürr, Science **320**, 1329 (2008).
- [27] F. Trimborn, D. Witthaut, and S. Wimberger, J. Phys. B **41**, 171001 (2008).
- [28] D. Witthaut, F. Trimborn, and S. Wimberger, Phys. Rev. Lett. **101**, 200402 (2008).
- [29] D. Witthaut, F. Trimborn, and S. Wimberger, Phys. Rev. A **79**, 033621 (2009).
- [30] V. S. Shchesnovich and V. V. Konotop Phys. Rev. A **81**, 053611 (2010).
- [31] E. M. Graefe, H. J. Korsch, and A. E. Niederle, Phys. Rev. Lett. **101**, 150408 (2008).
- [32] E. M. Graefe, H. J. Korsch, and A. E. Niederle, Phys. Rev. A **82**, 013629 (2010).
- [33] C. W. Gardiner and P. Zoller, Quantum Noise (Springer, Berlin, 2004).
- [34] S. H. Strogatz, Nonlinear Dynamics and Chaos (Addison-Wesley, New York, 1994).
- [35] W. E. Boyce and R. C. DiPrima, Elementary Differential Equations and Boundary Value Problems (Wiley, New York, 1997).
- [36] A. Smerzi, S. Fantoni, S. Giovanazzi, and S. R. Shenoy, Phys. Rev. Lett. **79**, 4950 (1997).
- [37] M. Albiez, R. Gati, J. Fölling, S. Hunsmann, M. Cristiani, and M. K. Oberthaler, Phys. Rev. Lett. **95**, 010402 (2005).